

## ***Supplementary Material***

# **Performance and Economic Analysis of Organosolv Softwood and Herbaceous Lignins to Activated Carbons as Electrode Materials in Supercapacitors**

**Lu Yu<sup>1,2</sup>, Kendhl Seabright<sup>1</sup>, Ishan Bajaj<sup>3</sup>, David J. Keffer<sup>2</sup>, David M. Alonso<sup>4</sup>, Chien-Te Hsieh<sup>5,\*</sup>, Mi Li<sup>1</sup>, Hao Chen<sup>6</sup>, Sheng Dai<sup>6,7</sup>, Yasser Ashraf Gandomi<sup>8</sup>, Christos T. Maravelias<sup>3,9</sup>, David P. Harper<sup>1,\*</sup>**

<sup>1</sup> Center for Renewable Carbon, Institute of Agriculture, The University of Tennessee, Knoxville, Tennessee 37996, United States

<sup>2</sup> Department of Materials Science and Engineering, The University of Tennessee, Knoxville, Tennessee 37996, United States

<sup>3</sup> Andlinger Center for Energy and the Environment, Princeton University, Princeton, NJ 08540, United States

<sup>4</sup> Glucan Biorenewables LLC, Madison, WI 53719, United States

<sup>5</sup> Department of Chemical Engineering and Materials Science, Yuan Ze University, Taoyuan 32003, Taiwan

<sup>6</sup> Department of Chemistry, The University of Tennessee, Knoxville, TN 37996, United States

<sup>7</sup> Chemical Sciences Division, Oak Ridge National Laboratory, Oak Ridge, TN 37831, United States

<sup>8</sup> Department of Chemical Engineering, Massachusetts Institute of Technology, Cambridge, MA 02142, United States

<sup>9</sup> Department of Chemical and Biological Engineering, Princeton University, Princeton, NJ 08540, United States

\* **Correspondence:** Prof. D.P. Harper (dharper4@utk.edu) and Prof. C.T. Hsieh ([cthsieh@saturn.yzu.edu.tw](mailto:cthsieh@saturn.yzu.edu.tw))

Table S1. Supercapacitor performance of activated carbons produced by various biomass materials.

Precursors	Activation method	Surface area ( $\text{m}^2 \text{ g}^{-1}$ )	Electrolyte	Specific capacitance	References
Coffee endocarp	$\text{CO}_2$	709	1 M $\text{H}_2\text{SO}_4$	176 F $\text{g}^{-1}$ at 10 mA	[1]
Corn husk	KOH	771	0.5 M $\text{H}_2\text{SO}_4$	314.83 F $\text{g}^{-1}$ at 1 mV $\text{s}^{-1}$	[2]
Corn syrup	Physical self-activation	1473	6 M KOH	168 F $\text{g}^{-1}$ at 0.2 A $\text{g}^{-1}$	[3]
Peanut shell	$\text{ZnCl}_2$	1565	6 M KOH	245 F $\text{g}^{-1}$ at 0.05 A $\text{g}^{-1}$	[4]
Kraft lignin	KOH	1148	6 M KOH	91.7 F $\text{g}^{-1}$ at 2 mV $\text{s}^{-1}$	[5]
Kraft lignin	steam & $\text{CO}_2$	591.7	2 M $\text{H}_2\text{SO}_4$	125.8 F $\text{g}^{-1}$ at 0.15A $\text{g}^{-1}$	[6]
Sugarcane bagasse	$\text{K}_2\text{CO}_3$	725	2 M KOH	265 F $\text{g}^{-1}$ at 0.2 A $\text{g}^{-1}$	[7]
GVL Lignin	steam & $\text{CO}_2$	1070	1 M $\text{H}_2\text{SO}_4$	367 at 0.1 mA $\text{cm}^{-2}$	this work

Table S2. Composition and elemental analysis of YP and SG lignin.

<b>Lignin</b>		<b>YP</b>	<b>SG</b>
<b>Purity</b>	ASL <sup>a</sup> +AIL <sup>b</sup>	96.60	94.04
	Ash	0.02	0.03
<b>Molecular weight</b>	$M_n$	2583	2238
	$M_w$	7747	6625
<b>Molar-mass dispersity (<math>D_M</math>)</b>	$M_w/M_n$	3.00	2.96
<b>Ultimate analysis (at.%)</b>	C	64.8	62.1
	H	6.3	6.1
	N	0.2	0.5
	O	28.7	31.3

<sup>a</sup> Acid-soluble lignin.

<sup>b</sup> Acid-insoluble lignin.

Table S3. Relative abundance of lignin linkages using  $^{13}\text{C}$ - $^1\text{H}$  NMR analysis.

	$\delta\text{C}/\delta\text{H}$ (ppm)	Label	Assignment	integral	
				SG	YP
	2.49/39.5	DMSO	Solvent	1.00	1.00
	103.9/6.65	$\text{S}_{2/6}$	$\text{C}_2/\text{H}_2$ and $\text{C}_6/\text{H}_6$ in etherified syringyl units (S)	0.849	--
	110.9/7.00	$\text{G}_2$	$\text{C}_2/\text{H}_2$ in guaiacyl units (G)	0.370	1.046
	115.1/6.72&6.98 and 118.7/6.77	$\text{G}_5/\text{G}_6$	$\text{C}_5/\text{H}_5$ and $\text{C}_6/\text{H}_6$ in guaiacyl units (G)	1.832	2.741
Lignin aromatic	114.8/6.73	$\text{H}_{3,5}$	$\text{C}_{3,5}/\text{H}_{3,5}$ in <i>p</i> -hydroxyphenyl units (H)	0.130	0.089
	127.8/7.20	$\text{H}_{2,6}$	$\text{C}_{2,6}/\text{H}_{2,6}$ in <i>p</i> -hydroxyphenyl units (H)	0.109	--
	115.5/6.72	$\text{PCA}_{3,5}$	$\text{C}_3/\text{H}_3$ and $\text{C}_5/\text{H}_5$ in p-coumarate (PCA)	1.030	0.259
	130.0/7.48	$\text{PCA}_{2,6}$	$\text{C}_2/\text{H}_2$ and $\text{C}_6/\text{H}_6$ in p-coumarate (PCA)	0.637	--
	113.5/6.27	$\text{PCA}_\beta$ and $\text{FA}_\beta$	$\text{C}_\beta/\text{H}_\beta$ in p-coumarate (PCA) and ferulate (FA)	0.273	0.033
	111.0/7.32	$\text{FA}_2$	$\text{C}_2/\text{H}_2$ in ferulic acid units (FA)	0.123	--
	123.0/7.10	$\text{FA}_6$	$\text{C}_6/\text{H}_6$ in ferulic acid units (FA)	0.040	0.134
	53.2/3.47	$\text{B}_\beta$	$\text{C}_\beta/\text{H}_\beta$ in $\beta$ -5' phenylcoumaran substructures (B)	0.045	0.145
Lignin aliphatic	53.6/3.07	$\text{C}_\beta$	$\text{C}_\beta/\text{H}_\beta$ in $\beta$ - $\beta'$ resinol substructures (C)	0.011	--
	55.5/3.75	OMe	C/H in methoxyls	8.233	8.202
	59.8/3.36 & 3.72	$\text{A}_\gamma$	$\text{C}_\gamma/\text{H}_\gamma$ in normal ( $\gamma$ -hydroxylated) $\beta$ -O-4' substructures (A)	1.142	0.862
	62.5/3.75	$\text{B}_\gamma$	$\text{C}_\gamma/\text{H}_\gamma$ in $\beta$ -5' phenylcoumaran substructures (B)	0.251	0.782
	71.2/3.80 & 4.17	$\text{C}_\gamma$	$\text{C}_\gamma/\text{H}_\gamma$ in $\beta$ - $\beta'$ resinol substructures (C)	0.028	--
	71.5/4.75	$\text{A}_\alpha/\text{A}'_\alpha$	$\text{C}_\alpha/\text{H}_\alpha$ in $\beta$ -O-4' substructures (A, A') -G & -S	0.257	0.156

Table S4. Pore structures of activated carbons prepared from YP and SG lignin precursors.

Carbon type	Specific surface area		Pore volume		
	$S_{\text{BET}}$ ( $\text{m}^2 \text{ g}^{-1}$ )	$S_{\text{BJH}}$ ( $\text{m}^2 \text{ g}^{-1}$ )	$V_t$ ( $\text{cm}^3 \text{ g}^{-1}$ )	$V_{\text{micro}}$ (%)	$V_{\text{meso}}$ (%)
YP-AC	1070	467	1.27	56	44
SG-AC	507	56	0.29	89	11

$S_{\text{BET}}$ : Specific surface area computed using BET equation.

$S_{\text{BJH}}$ : Specific surface area computed using BJH equation.

$V_t$ : Total pore volume estimated at a relative pressure of 0.98.

$V_{\text{micro}}$ : Micropore volume determined from  $t$ -plot method.

$V_{\text{meso}}$ : Mesopore volume determined from the subtraction of micropore volume from total pore volume.

Table S5. Material flow rate of the main streams based on the process flow diagram shown in Figure 10 and the energy consumption of the process areas.

Areas	Streams	Temperature (°C)	Pressure (atm)	Flow rate (tonne/h)		Energy requirement (MW)	
				YP bioref.	SG bioref.	YP bioref.	SG bioref.
	1	25	1	0.31	0.2		
	2	25	1	9.5	6.9		
	3	25	1	17.5	12.7		
	4	144.8	3.4	34.1	24.8		
A100	5	144.8	3.4	53.6	38.9	Electricity:	
	6	125	3.4	41.8	30.4	0.004	0.003
	7	153.6	1	33.9	24.7		
	25	194.7	1	9.1	5.2		
	8	149.8	4.5	215.7	157.0	Cooling:	
	9	149.8	4.5	212.1	154.4	7.4	5.3
A200	10	149.8	4.5	34.9	25.4	Electricity:	
	14	25	1	0.4	0.3	3.1	2.2
	17	138.5	3.4	4.9	3.6		
	18	138.5	3.4	0.4	0.3		
	11	25	1	0.1	0.1	Heating:	
	12	167.7	1.2	0.9	1.9	8.5	6.2
A300	13	25	1	0.09	0.07	Cooling:	
	15	208	1	24.9	18.1	9.7	7.1
	16	208	1	3.8	1.5	Electricity:	
	19	25	1	0.6	0.4	0.021	0.015
	20	800	1	3.6	2.6		
	21	800	1	0.2	0.1	Heating:	
A400	22	25	1	0.06	0.04	2.3	1.8
	23	800	1.5	0.2	0.1	Electricity:	
	24	800	1.5	0.1	0.1	0.4	0.3

Table S6. Detailed capital costs of the equipment in A400.

Equipment	Quantity	Equipment installed costs (Million \$)		Source
		YP biorefinery	SG biorefinery	
Air separation unit	1	2.2	28.2	[8]
Fluidized bed reactor	3	2.9	30.1	[9]
Cyclone	3	0.1	5.5	Aspen Plus
Ball Mill	1	0.07	4.6	Aspen Plus
Compressor	3	0.6	20.6	[10]

Table S7. A summary of equipment installed costs of different process areas.

Area	Capital costs (Million \$)	
	YP biorefinery	SG biorefinery
A100	34.2	28.2
A200	36.4	30.1
A300	6.7	5.5
A400	5.9	4.6
A500	24.9	20.6
A600	8.0	6.6
A700	2.7	2.3
A800	1.9	1.5

Table S8. Summary of cost components for YP- and SG-based biorefineries.

Cost components	Costs (Million \$)	
	YP biorefinery	SG biorefinery
Inside-battery-limits (ISBL)	83.1	68.4
equipment costs (A100-A400)		
Outside-battery-limits (OSBL)	37.5	31.0
equipment costs (A500-A800)		
Warehouse	4.0% of ISBL	3.3
Site development	9.0% of ISBL	7.5
Additional piping	4.5% of ISBL	3.8
<b>Total direct costs (TDC)</b>	<b>135.2</b>	<b>111.4</b>
Prorateable expenses	10.0% of TDC	13.5
Field expenses	10.0% of TDC	13.5
Home office and construction fee	20.0% of TDC	27.0
Project contingency	40.0% of TDC	13.5
Other costs (start-up, permits, etc.)	10.0% of TDC	13.5
<b>Total indirect costs</b>	<b>81.0</b>	<b>66.9</b>
<b>Fixed capital investment (FCI)</b>	<b>216.2</b>	<b>178.3</b>
Land		1.9
Working capital	5.0% of FCI	10.8
<b>Total capital investment (TCI)</b>	<b>228.9</b>	<b>189.1</b>

Table S9. Summary of material prices and sources.

Component	Price (\$/ton)	Source
YP	70	[4]
SG	80	[4]
H <sub>2</sub> SO <sub>4</sub>	86	[5]
GVL	1000	[6]
NaCl	182	USGS
Heavy oil	330	Baytex energy
Lime	237	[4]
CO <sub>2</sub>	70	[7]
Boiler chemicals	5950	[4]
Cooling tower chemicals	3565	[4]
WWT nutrients	5251	[4]

Table S10. Financial assumptions.

Plant life	30 years
Capacity factor	90% (7884 hr/year)
Internal rate of return	30%
Plant depreciation	7 years
Loan terms	10-year loan at 8% APR
Construction time	3 years
Financing	40% equity
Federal tax rate	21%
First 12 months' expenditure	8%
Second 12 months' expenditure	60%
Last 12 months' expenditure	32%
Start-up time	6 months
Working capital	5% of fixed capital investment
Revenue during start-up	50%
Variable operating costs during start-up	75%
Fixed operating costs during start-up	100%

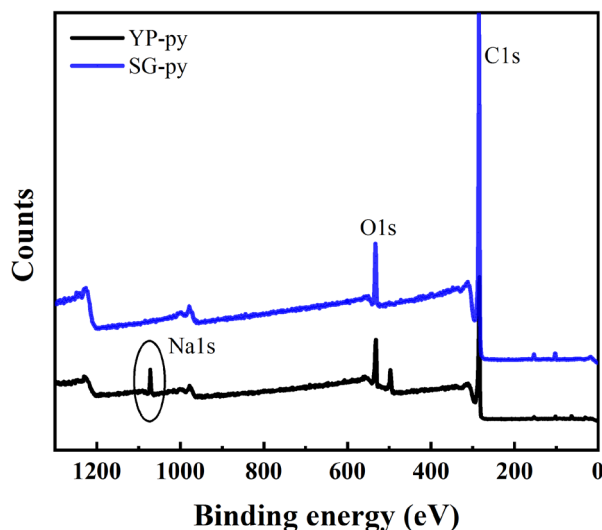


Figure S1. Survey-scan XPS spectra of YP-py and SG-py samples.

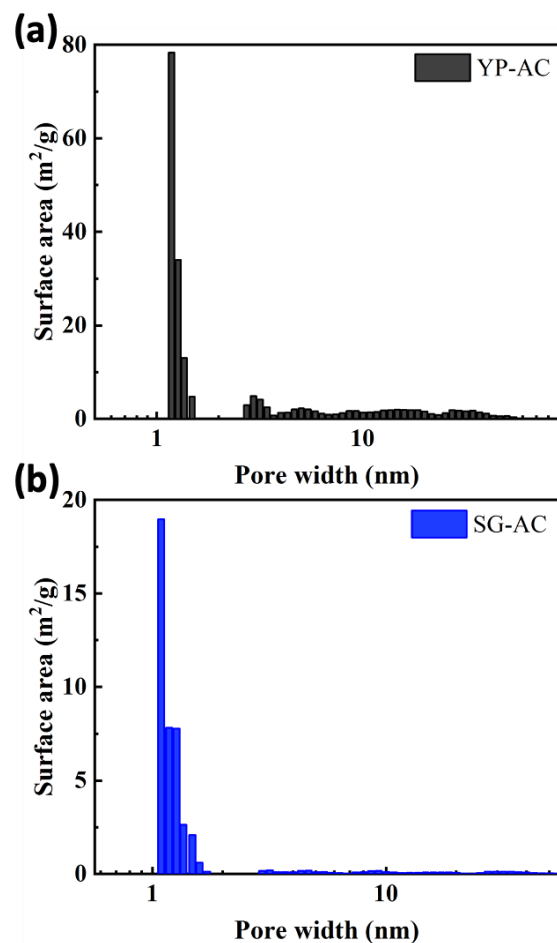


Figure S2. Pore size distributions of activated carbons prepared from (a) YP and (b) SG lignin precursors.

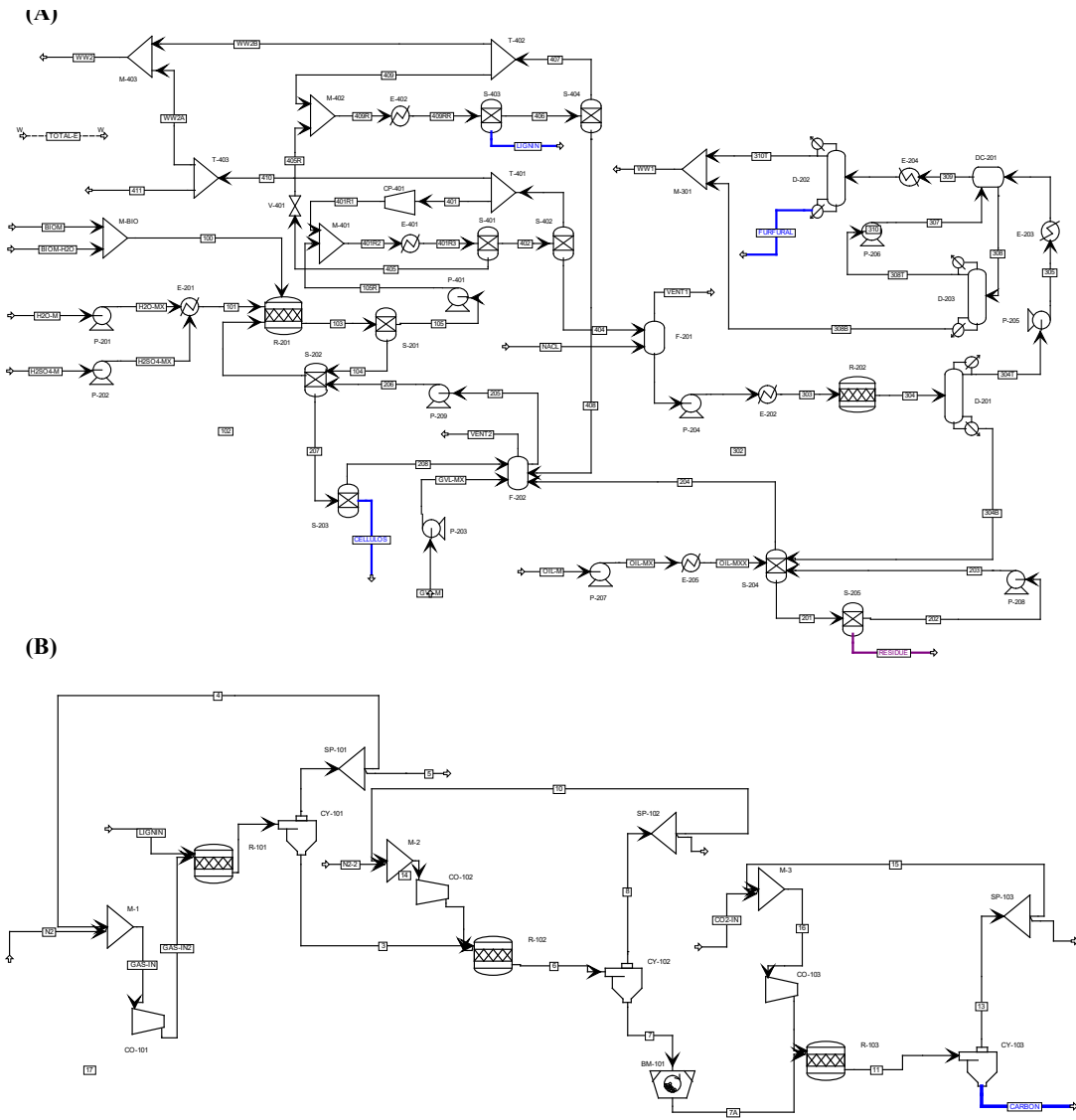


Figure S3. Aspen Plus model for (A) A100-A300 and (B) A400.

## References

- [1] Valente Nabais, JM, Teixeira, JG, Almeida, I. 2011. Development of easy made low cost bindless monolithic electrodes from biomass with controlled properties to be used as electrochemical capacitors. *Bioresour Technol*, 102, 2781–2787. <https://doi:10.1016/j.biortech.2010.11.083>
- [2] Surya K, Michae, MS. Novel interconnected hierarchical porous carbon electrodes derived from bio-waste of corn husk for supercapacitor applications. *J Electroanal Chem*, 2020; 878, 114674. <https://doi:10.1016/j.jelechem.2020.114674>
- [3] Wenxin C, FuqianY. Supercapacitors from high fructose corn syrup-derived activated carbons. *Mater Today Energy*, 2018; 9, 406-415.

- <https://doi.org/10.1016/j.mtener.2018.07.002>
- [4] He, X., Ling, P., Qiu, J., Yu, M., Zhang, X., Yu, C., Zheng, M., 2013. Efficient preparation of biomass-based mesoporous carbons for supercapacitors with both high energy density and high power density. *Journal of Power Sources* 240, 109–113. <https://doi:10.1016/j.jpowsour.2013.03.174>
  - [5] Guo, N., Li, M., Sun, X., Wang, F., Yang, R., 2017. Enzymatic hydrolysis lignin derived hierarchical porous carbon for supercapacitors in ionic liquids with high power and energy densities. *Green Chemistry* 19, 2595–2602. <https://doi:10.1039/c7gc00506g>
  - [6] Yu, L., Hsieh, C.-T., Keffer, D.J., Chen, H., Goenaga, G.A., Dai, S., Zawodzinski, T.A., Harper, D.P., 2021. Hierarchical Lignin-Based Carbon Matrix and Carbon Dot Composite Electrodes for High-Performance Supercapacitors. *ACS Omega* 6, 7851–7861. <https://doi:10.1021/acsomega.1c00448>
  - [7] Subhajit S, Anil A, Umesh KG, Anurag G. Investigations on porous carbon derived from sugarcane bagasse as an electrode material for supercapacitors. *Biomass Bioenergy*, 2020; 142,105730. <https://doi.org/10.1016/j.biombioe.2020.105730>
  - [8] Hamelinck CN, Faaij APC. Future prospects for production of methanol and hydrogen from biomass. *J Power Sources* 2002;111:1–22. [https://doi.org/10.1016/S0378-7753\(02\)00220-3](https://doi.org/10.1016/S0378-7753(02)00220-3).
  - [9] Swanson RM, Platon A, Satrio JA, Brown RC. Techno-economic analysis of biomass-to-liquids production based on gasification scenarios. 2010.
  - [10] Seider, Warren D.; Seader, J.D.; Lewin, Daniel R.; Widagdo S. Product and Process Design Principles: Synthesis, Analysis and Evaluation. 3rd ed. Wiley; 2009.
  - [11] Gonzalez R, Daystar J, Jett M, Treasure T, Jameel H, Venditti R, et al. Economics of cellulosic ethanol production in a thermochemical pathway for softwood, hardwood, corn stover and switchgrass. *Fuel Process Technol* 2012;94:113–22. <https://doi.org/10.1016/j.fuproc.2011.10.003>.
  - [12] Davis R, Grundl N, Tao L, Biddy MJ, Tan ECD, Beckham GT, et al. Process Design and Economics for the Conversion of Lignocellulosic Biomass to Hydrocarbon Fuels and Coproducts: 2018 Biochemical Design Case Update: Biochemical Deconstruction and Conversion of Biomass to Fuels and Products via Integrated Biorefinery Path. 2018.
  - [13] Alonso DM, Hakim SH, Zhou S, Won W, Hosseinaei O, Tao J, et al. Increasing the revenue from lignocellulosic biomass: Maximizing feedstock utilization. *Sci Adv* 2017;3. <https://doi.org/10.1126/sciadv.1603301>.

- [14] Jouny M, Luc W, Jiao F. General Techno-Economic Analysis of CO<sub>2</sub> Electrolysis Systems. *Ind Eng Chem Res* 2018;57:2165–77.  
<https://doi.org/10.1021/acs.iecr.7b03514>.